CE: PA
QC: SS

Biological Journal of the Linnean Society, 2018, **XX**, 1–13. With 2 figures.

High rate of meiotic recombination and its implications for intricate speciation patterns in the white wagtail (*Motacilla alba*)

GEORGY A. SEMENOV,[1,2,*] EKATERINA A. BASHEVA,[3] PAVEL M. BORODIN,[3,4] and ANNA A. TORGASHEVA[2,3,4]

[1]*Ecology and Evolutionary Biology, University of Colorado, N315/317 Ramaley Hall, Boulder, CO 80309, USA*
[2]*Institute of Systematics and Ecology of Animals, Frunze 11, Novosibirsk 630091, Russian Federation*
[3]*Institute of Cytology and Genetics, Siberian Branch of Russian Academy of Sciences, Lavrentiev Ave. 10, Novosibirsk 630090, Russian Federation*
[4]*Novosibirsk State Research University, Department of Cytology and Genetics, Pirogova st. 4, Novosibirsk 630090, Russian Federation*

Received 18 June 2018; revised 12 August 2018; accepted for publication 13 August 2018

Conspicuous phenotypic differences sometimes coexist with shallow genome-wide divergence between taxa. Along with genomically localized selection and extensive gene flow, a high rate of meiotic recombination might contribute to such a pattern; however, empirical evidence for the latter is lacking. We studied meiotic recombination in the white wagtail (*Motacilla alba*) – a bird species showing extensive divergence in plumage traits but little genomic differentiation, yet broadly incongruent geographical variation between morphological traits and genetic markers. We found that the white wagtail ($2n = 82$) has the highest number of recombination nodules per autosome set (76.1 ± 8.6) and thus the longest autosomal genetic map (3805 cM) among all birds examined to date. We suggest that a high recombination rate could promote decoupling of phenotypic and genetic variation and influence the genetic architecture of traits involved in reproductive barriers. Our study highlights the importance of studying meiotic recombination within a unified methodological framework, and the need for a broader sampling of taxa to understand how variation in recombination rates contributes to patterns of speciation.

ADDITIONAL KEYWORDS: crossing over – MLH1 – recombination – speciation – synaptonemal complex.

INTRODUCTION

Variation in meiotic recombination – such as differences in the frequency and genomic distribution of crossover events – has fundamental effects on evolutionary processes (Stapley *et al.*, 2017a). These characteristics shape associations between alleles at independent loci, thereby influencing the rate of evolutionary responses, the fate of new beneficial mutations and the effectiveness of selection against deleterious mutations (Muller, 1964; Hill & Robertson, 1966; Kondrashov, 1988; Butlin, 2005; Haddrill *et al.*, 2007; Dumont & Payseur, 2008). Recombination rates vary broadly across populations, species and higher taxonomic levels, suggesting that they may contribute globally to patterns of biological diversification (Stapley *et al.*, 2017b).

Of particular note, recombination characteristics can directly influence the processes of population divergence and speciation (Coyne & Orr, 2004; Butlin, 2005; Ortiz-Barrientos *et al.*, 2016; Payseur, 2016). We might therefore expect variation in recombination rates to contribute to distinct speciation patterns observed across taxa. For instance, extensive morphological diversification sometimes coexists with shallow genetic divergence between populations. Several examples are known in birds, where striking plumage differences are characterized by little or no differentiation in molecular markers throughout most of their genomes [e.g. *Vermivora* warblers (Toews *et al.*, 2016),

*Corresponding author. E-mail: georgy.semenov@colorado.edu

Sporophila seedeaters (Campagna *et al.*, 2017), *Corvus* crows (Poelstra *et al.*, 2014) and *Lonchura* munias (Stryjewski & Sorenson, 2017)]. Selection promoting or maintaining divergence at a few key genomic regions and gene flow homogenizing selectively neutral variation are considered the major drivers of such patterns (e.g. Poelstra *et al.*, 2014). Yet, crossover frequency and distribution determine which traces selection and gene flow leave in genomic landscapes (Wolf & Ellegren, 2017). All else being equal, a high recombination rate will slow down the process of lineage sorting, with the exception of non-recombinant genomic regions such as mitochondrial DNA (mtDNA) and differential regions of Y and W chromosomes (Pease & Hahn, 2013), and shrink the size of haplotype blocks affected by linked selection, leading to highly localized effects of selection across the genome (Dumont & Payseur, 2008; Nosil & Feder, 2012; Cutter & Payseur, 2013; Feder *et al.*, 2013). It is therefore plausible that a pattern of marked phenotypic diversification coexisting with a lack of genome-wide divergence can be associated with high recombination rates. However, empirical support for this connection has yet to be found. Absence of this evidence might be due in particular to a lack of comparative data on recombination patterns in many taxonomic groups and the substantial bias of recombination research towards a handful of model organisms (Stapley *et al.*, 2017b).

The white wagtail (*Motacilla alba* Linnaeus, 1758) is a widespread passerine bird (Fig. 1). Population structure and differentiation in molecular markers in this species are broadly incongruent with geographical variation in plumage signals – a pattern that was appropriately named 'messy speciation' in a recent review of literature pertaining to speciation genomics (Campbell *et al.*, 2018). Four divergent mtDNA lineages have been discovered across the white wagtail range, with two clades restricted to (1) Morocco and (2) a few localities in the Caucasus, Central Asia and British Isles (Pavlova *et al.*, 2005; Li *et al.*, 2016; Semenov *et al.*, 2017). Two other widespread mtDNA clades are distributed across (3) northern Eurasia and (4) central to south-eastern Eurasia, respectively, and have an average sequence difference of 0.4%, corresponding to a split at 0.31–0.33 Mya (Pavlova *et al.*, 2005; Li *et al.*, 2016). Population structure in microsatellite (Semenov *et al.*, 2018) and single nucleotide polymorphism (SNP) markers (Harris *et al.*, 2018) is to some extent consistent with that of mtDNA, with two major population clusters spanning northern and south-eastern Eurasia. However, differentiation in nuclear markers is shallow compared to that in mtDNA. Most estimates of pairwise genetic differentiation based on microsatellite markers were low and non-significant between remote north Eurasian subspecies (Semenov *et al.*, 2018), contrasting with estimates from mtDNA (Pavlova *et al.*, 2005). In addition, terminal samples from a 3000-km transect between *alba* and *personata* subspecies had less than 1% of loci with allele frequency differences exceeding 0.4 and no alleles fixed to alternative states among ~20 000 nuclear SNPs (Semenov *et al.*, 2017), suggesting a very low level of genome-wide differentiation. With the exception of the Moroccan-distributed subspecies *subpersonata*, each of the genetically delineated populations encompasses several subspecies with distinct plumage. Moreover, geographical locations of contact zones between genetic clusters, inferred from both nuclear and mtDNA markers, do not coincide with the regions where plumage-delineated subspecies come into contact, with the only known exception occurring in eastern Russia (Pavlova *et al.*, 2005; Semenov *et al.*, 2018).

A study of the hybrid zone between *alba* and *personata* subspecies revealed that wagtails mate assortatively with respect to head plumage coloration (Semenov *et al.*, 2017). However, selection associated with this assortative mating probably targets a very small fraction of the genome, with no evidence for reproductive barriers in molecular markers (Semenov *et al.*, 2017). Although little is known about patterns in other hybrid zones, repetitive divergence in several plumage hotspots (head and neck sides, wing and back colour) suggests a role of plumage divergence in promoting speciation (Semenov *et al.*, 2018). Previous studies concluded that the white wagtail subspecies (1) have undergone recent and rapid divergence with selection mostly focused on a few plumage genes, (2) probably have a long history of gene flow and (3) have experienced periods of repeated contact and subsequent isolation during Pleistocene climate fluctuations (Pavlova *et al.*, 2005; Li *et al.*, 2016; Harris *et al.*, 2018; Semenov *et al.*, 2018). These processes could collectively result in substantial decoupling between patterns observed in plumage traits and molecular markers. Here, we studied meiotic recombination in the white wagtail and assessed its potential contribution to this striking disparity between phenotypic and molecular variation.

Meiotic recombination can be estimated by linkage mapping, using genome-wide patterns of linkage disequilibrium, or through cytological methods. Linkage mapping requires controlled crosses or known pedigrees and to a large extent is restricted to model organisms (Boopathi, 2013). Furthermore, its resolution depends critically on the number and distribution of genetic markers, where low marker density and the location of markers in regions of low recombination can lead to an underestimation of the recombination rate. Estimation of recombination rates using genome-wide linkage disequilibrium (Mueller, 2004) has been increasingly applied in recent years (Singhal *et al.*, 2015; Kawakami *et al.*, 2017). Despite the fine

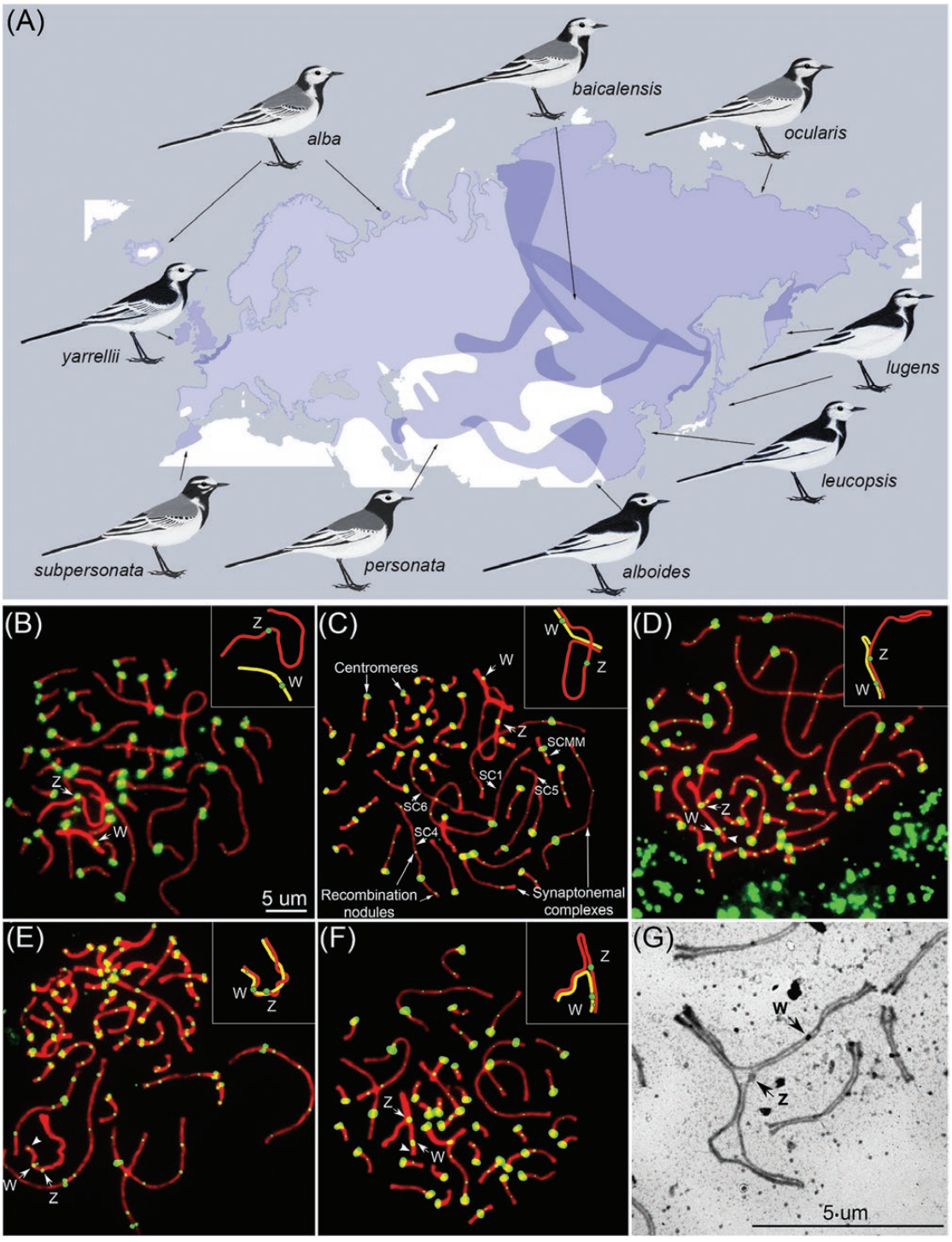

Figure 1. A, plumage variation and geographical distribution of the white wagtail; darker areas are zones of hybridization between the subspecies. B–F, white wagtail ovary cell spreads immunostained for SCs (red), recombination nodules (small green dots) and centromeres (large green) (see C for a labelled example). Arrows in B–F indicate centromeres of Z and W chromosomes and arrowheads indicate their recombination nodules. Cartoon insertions show pattern of ZW synapsis. SC1, 4, 5, 6 and SCMM are five autosomal SCs that were reliably identifiable across cells based on relative size and centromere location (see Fig. 2 for their recombination landscapes). G, fragment of an electron microphotograph (silver staining) showing complete synapsis of whole W and Z chromosomes folded in the medial part at the synaptic configuration similar to that shown in F.

resolution that this method offers, the resulting estimates depend on sequencing coverage of the genome, which varies broadly across studies, complicating comparative inference. The cytological approach we adopt here utilizes immunostaining to visualize recombination patterns on meiotic cell spreads. Cytological assays can be used to detect recombination nodules [multicomponent proteinaceous structures that occur at crossover sites at the pachytene stage of meiosis (Stack & Anderson, 2002)], synaptonemal complexes (SCs) [the protein structures that form during meiosis and indicate paired sister chromatids (Westergaard & von Wettstein, 1972)] and the position of centromeric chromosomal regions [the specialized DNA sequences that link pairs of sister chromatids (Pluta *et al.*, 1995)]. Cytological methods allow precise estimation of the overall number and distribution of crossover events along chromosomes (Anderson *et al.*, 1999) and, unlike other methods, permit direct comparison between independent studies (Veller & Nowak, 2017).

MATERIAL AND METHODS

Three female nestlings of *Motacilla alba alba* were collected from the same nest 3–5 days after hatching in the Novosibirsk district, Russia (55.329766°N, 79.056258°E).

Oocyte spreads were prepared from ovaries using a drying-down technique (Peters *et al.*, 1997). Spreads for electron microscopy were stained with silver nitrate (Howell & Black, 1980) and covered with plastic film. After light microscopic examination, spreads were transferred to specimen grids and examined with an electron microscope JEM-100 (Jeol) at 80 kV. Immunostaining was performed according to Anderson *et al.* (1999) with rabbit polyclonal primary antibodies to SYCP3 (1:500 dilution; ab150292, Abcam), mouse monoclonal antibodies to MLH1 (1:50; ab14206, Abcam), and human anti-centromere antibodies (ACA) (1:100, Cat#15-235-0001, Antibodies Inc.). We used Cy3-conjugated goat anti-rabbit (1:500; Cat#111-165-144, Jackson ImmunoResearch), fluorescein isothiocyanate (FITC)-conjugated goat anti-mouse (1:50; Cat#115-095-003, Jackson ImmunoResearch) and FITC-conjugated donkey anti-human (1:100, Cat#709-095-149, Jackson ImmunoResearch) secondary antibodies. Antibodies were diluted in PBT (3% bovine serum albumin, 0.1% Tween 20 in PBS). A solution of 10% PBT was applied for 45 min to block the reaction. Spreads were incubated with primary antibodies overnight in a humid chamber at 37 °C and for 1 h at 37 °C with secondary antibodies. Slides were mounted in Vectashield (Vector Laboratories). The assays were visualized with an Axioplan2 imaging microscope (Carl Zeiss) using a CCD camera (CV M300, JAI), CHROMA filter sets and the ISIS4 image-processing package (MetaSystems GmbH). Brightness and contrast of all images were enhanced using Corel PaintShop Photo Pro X6 (Corel Corp.).

The centromeres were identified based on ACA foci. They differed from the MLH1 signal by brighter and more diffuse staining (Fig. 1B–F). MLH1 signals were only scored if they were localized on SCs. The length of the SC of each chromosome arm was measured in micrometres and the positions of centromeres and MLH1 foci in relation to the centromere were recorded using MicroMeasure 3.3 (Reeves, 2001). To generate recombination maps, we calculated the absolute position of each MLH1 focus by multiplying the relative position of each focus by the average absolute length for the chromosome arm. These data were pooled for each arm and plotted to represent a recombination map. To estimate the length of the recombination map in centimorgans (cM), we multiplied the average number of MLH1 foci per cell by 50 map units (one recombination event = 50 cM). The Statistica 6.0 software package (StatSoft) was used for descriptive statistics. Values in the text and table are presented as means ± SD.

RESULTS

We analysed 11 119 MLH1 foci at 5880 completely paired autosomal SCs in 147 oocytes. The karyotypes of the white wagtail contained 40 SCs and the ZW pair ($2n$ = 82; the fundamental number of chromosomal arms FN = 94). The mean total length of the SCs (182.7 ± 19.2 μm) was comparable to that of other birds (Table 1). The number of MLH1 foci per cell (76.1 ± 8.6) and per micrometre of SC (0.42), and the genetic map length (3805 cM) were the highest among all birds studied to date (Table 1).

We identified individual SCs by their relative lengths and centromeric indices, and the ZW pair as the only heteromorphic SC. SC2 and SC3 were large submetacentrics similar in sizes and centromeric indices. The macroSCs 7–10 and all microSCs except one were acrocentric, with chromosomal sizes gradually decreasing in length. The size rank of SCMM varied between cells from 16th to 20th. Four macrochromosomal SCs and one microchromosomal SC were readily identifiable across assays: SC1 was the largest metacentric, SC4 was a large submetacentric, SC5 was a large subtelocentric, SC6 was a large acrocentric and SCMM was the only metacentric microchromosome (Fig. 1C). These SCs were used to assess recombination distributions along chromosomal arms (Fig. 2). Autosomal SCs showed pronounced distal recombination peaks, although MLH1 foci were present in all parts of the

Table 1. Meiotic recombination features of bird species examined to date

Common name	Latin name	Order	Family	Method	Sex	2*n*	Recombination nodules per autosome set		Genetic map (cM)	Autosomal SC length (μm)		MLH1 per μm SC	Reference
							X	SD		*X*	*SD*		
White wagtail	*Motacilla alba*	Passeriformes	Motacillidae	Cytological	F	82	76.1	8.6	3805	183	19	0.42	This study
Greater rhea	*Rhea americana*	Rheiformes	Rheidae	Cytological	F	80	58.8	4.4	2940	279	37	0.21	(del Priore & Pigozzi, 2017)
Greylag goose	*Anser anser*	Anseriformes	Anatidae	Cytological	F	80	72.6	7.8	3632	283	41	0.26	(Torgasheva & Borodin, 2017)
Greylag goose	*Anser anser*	Anseriformes	Anatidae	Cytological	M	80	57.9	7.6	2897	281	40	0.21	(Torgasheva & Borodin, 2017)
Domestic duck (mallard)	*Anas platyrhynchos*	Anseriformes	Anatidae	Cytological	F	80	55.9	3.8	2795	NA	NA	NA	(Pigozzi & del Priore, 2016)
Domestic duck (mallard)	*Anas platyrhynchos*	Anseriformes	Anatidae	LinkageMap	SA	80	NA	NA	1766	NA	NA	NA	(Huang *et al.*, 2009)
Domestic chicken	*Gallus domesticus*	Galliformes	Phasianidae	Cytological	F	78	65.2	4.0	3260	163	NA	0.4	(Pigozzi, 2001)
Domestic chicken	*Gallus domesticus*	Galliformes	Phasianidae	LinkageMap	F	78	NA	NA	3098	NA	NA	NA	(Groenen *et al.*, 2009)
Domestic chicken	*Gallus domesticus*	Galliformes	Phasianidae	LinkageMap	M	78	NA	NA	3145	NA	NA	NA	(Groenen *et al.*, 2009)
Domestic chicken	*Gallus domesticus*	Galliformes	Phasianidae	LinkageMap	SA	78	NA	NA	3228	NA	NA	NA	(Groenen *et al.*, 2009)
Domestic chicken	*Gallus domesticus*	Galliformes	Phasianidae	LinkageMap	SA	78	NA	NA	2763	NA	NA	NA	(Pengelly *et al.*, 2016)
Japanese quail	*Coturnix japonica*	Galliformes	Phasianidae	Cytological	F	78	55.3	2.1	2765	239	34	0.23	(Calderón & Pigozzi, 2006)
Japanese quail	*Coturnix japonica*	Galliformes	Phasianidae	Cytological	M	78	56.3	1.8	2815	231	29	0.24	(Calderón & Pigozzi, 2006)
Japanese quail	*Coturnix japonica*	Galliformes	Phasianidae	LinkageMap	SA	78	NA	NA	2816	NA	NA	NA	(Kikuchi *et al.*, 2005)
Zebra finch	*Taeniopygia guttata*	Passeriformes	Estrildidae	Cytological	F	78	45.7	0.4	2285	154	25	0.30	(Calderón & Pigozzi, 2006)
Zebra finch	*Taeniopygia guttata*	Passeriformes	Estrildidae	Cytological	M	78	45.2	0.2	2260	141	9	0.32	(Calderón & Pigozzi, 2006)
Zebra finch	*Taeniopygia guttata*	Passeriformes	Estrildidae	LinkageMap	SA	78	NA	NA	1341	NA	NA	NA	(Backström *et al.*, 2010)
Zebra finch	*Taeniopygia guttata*	Passeriformes	Estrildidae	LinkageMap	SA	78	NA	NA	1068	NA	NA	NA	(Stapley *et al.*, 2008)
Black tern	*Chlidonias niger*	Charadriiformes	Laridae	Cytological	F	68	43.1	5.0	2155	238	39	0.18	(Lisachov *et al.*, 2017)
Common tern	*Sterna hirundo*	Charadriiformes	Laridae	Cytological	F	74	52.0	4.2	2600	288	47	0.18	(Lisachov *et al.*, 2017)
Eurasian hobby	*Falco subbuteo*	Falconiformes	Falconidae	Cytological	M	50	51.1*	6.6	2555	258*	50	0.20	(Malinovskaya *et al.*, 2018)
Common swift	*Apus apus*	Apodiformes	Apodidae	Cytological	M	78	51.4*	4.3	2570	208*	32	0.25	(Malinovskaya *et al.*, 2018)
Domestic pigeon	*Columba livia*	Columbiformes	Columbidae	Cytological	F	80	62.7	4.9	3135	228	22	0.28	(Pigozzi & Solari, 1999b)
Domestic pigeon	*Columba livia*	Columbiformes	Columbidae	Cytological	M	80	64.7	4.8	3235	248	21	0.26	(Pigozzi & Solari, 1999a)
Domestic turkey	*Meleagris gallopavo*	Galliformes	Phasianidae	LinkageMap	F	80	NA	NA	2077	NA	NA	NA	(Aslam *et al.*, 2010)

Table 1. *Continued*

Common name	Latin name	Order	Family	Method	Sex	2*n*	Recombination nodules per autosome set		Genetic map (cM)	Autosomal SC length (μm)		MLH1 per μm SC	Reference
							X	SD		*X*	*SD*		
Domestic turkey	*Meleagris gallopavo*	Galliformes	Phasianidae	LinkageMap	M	80	NA	NA	2431	NA	NA	NA	(Aslam *et al.*, 2010)
Domestic turkey	*Meleagris gallopavo*	Galliformes	Phasianidae	LinkageMap	SA	80	NA	NA	2324	NA	NA	NA	(Aslam *et al.*, 2010)
Great tit	*Parus major*	Passeriformes	Paridae	LinkageMap	SA	78	NA	NA	2600	NA	NA	NA	(Van Oers *et al.*, 2014)
Great tit	*Parus major*	Passeriformes	Paridae	LinkageMap	SA	78	NA	NA	2700	NA	NA	NA	(Van Oers *et al.*, 2014)
Eurasian blue tit	*Cyanistes caeruleus*	Passeriformes	Paridae	LinkageMap	F	NA	NA	NA	1046	NA	NA	NA	(Hansson *et al.*, 2010)
Eurasian blue tit	*Cyanistes caeruleus*	Passeriformes	Paridae	LinkageMap	M	NA	NA	NA	887	NA	NA	NA	(Hansson *et al.*, 2010)
Eurasian blue tit	*Cyanistes caeruleus*	Passeriformes	Paridae	LinkageMap	SA	NA	NA	NA	935	NA	NA	NA	(Hansson *et al.*, 2010)
Siberian jay	*Perisoreus infaustus*	Passeriformes	Corvidae	LinkageMap	F	NA	NA	NA	998	NA	NA	NA	(Jaari *et al.*, 2009)
Siberian jay	*Perisoreus infaustus*	Passeriformes	Corvidae	LinkageMap	M	NA	NA	NA	774	NA	NA	NA	(Jaari *et al.*, 2009)
Siberian jay	*Perisoreus infaustus*	Passeriformes	Corvidae	LinkageMap	SA	NA	NA	NA	863	NA	NA	NA	(Jaari *et al.*, 2009)
Great reed warbler	*Acrocephalus arundinaceus*	Passeriformes	Acrocephalidae	LinkageMap	F	80	NA	NA	858	NA	NA	NA	(Åkesson *et al.*, 2007)
Great reed warbler	*Acrocephalus arundinaceus*	Passeriformes	Acrocephalidae	LinkageMap	M	80	NA	NA	552	NA	NA	NA	(Åkesson *et al.*, 2007)
Great reed warbler	*Acrocephalus arundinaceus*	Passeriformes	Acrocephalidae	LinkageMap	SA**	80	NA	NA	2000	NA	NA	NA	(Åkesson *et al.*, 2007)
Collared flycatcher	*Ficedula albicollis*	Passeriformes	Muscicapidae	LinkageMap	F	NA	NA	NA	1627	NA	NA	NA	(Backström *et al.*, 2008)
Collared flycatcher	*Ficedula albicollis*	Passeriformes	Muscicapidae	LinkageMap	M	NA	NA	NA	1982	NA	NA	NA	(Backström *et al.*, 2008)
Collared flycatcher	*Ficedula albicollis*	Passeriformes	Muscicapidae	LinkageMap	SA	NA	NA	NA	1787	NA	NA	NA	(Backström *et al.*, 2008)
Collared flycatcher	*Ficedula albicollis*	Passeriformes	Muscicapidae	LinkageMap	SA	NA	NA	NA	3132	NA	NA	NA	(Kawakami *et al.*, 2014)
Song sparrow	*Melospiza melodia*	Passeriformes	Passerellidae	LinkageMap	NA	NA	NA	NA	1731	NA	NA	NA	(Nietlisbach *et al.*, 2015)

X, average; SD, standard deviation; SA, sex average; 2*n* = diploid chromosomal set.
*The ZZ SCs were not identified and excluded from total MLH1 count and SC length.
†Expected sex average.

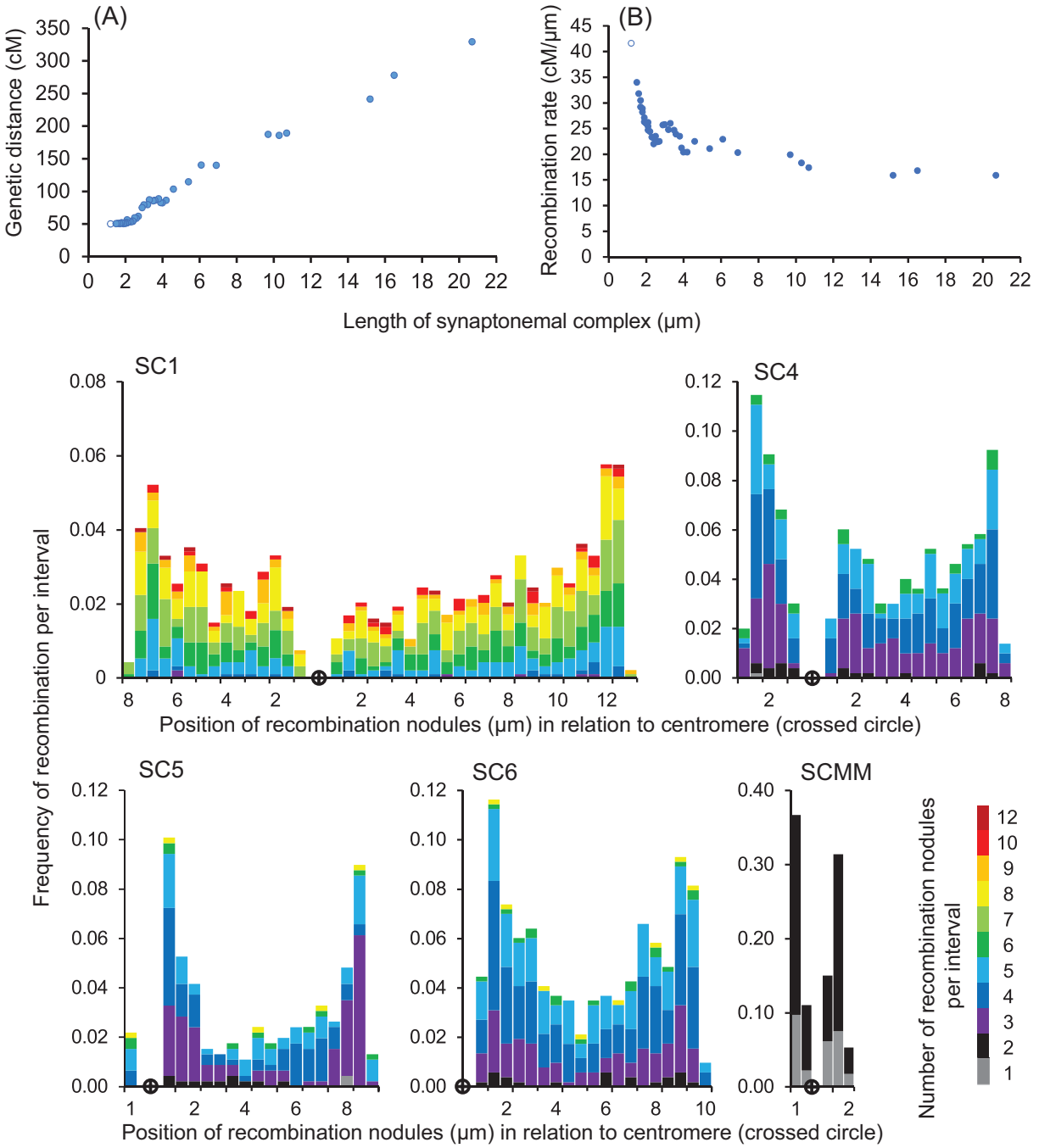

Figure 2. Top: the relationship between (A) genetic distance and synaptonemal complex length and (B) recombination rate and synaptonemal complex length. Open circles show the pseudoautosomal region of the ZW chromosome synaptonemal complex. Middle and bottom: distribution of recombination nodules along the arms of four macrochromosomes (SC1, 4, 5 and 6) and one microchromosome (SCMM). Colours indicate bivalents with 1–12 MLH1 foci per bivalent (see scale).

bivalents (Fig. 2). MLH1 frequency was lower in very narrow pericentromeric regions (about 1 μm in SC1 and SC5). The long arms of some macrobivalents (SC4, SC5, SC6) showed a clear secondary peak in the proximal regions. In SC6, the proximal peak of recombination was even more pronounced than the distal peak.

Across all SCs, there was a positive linear relationship between SC length and genetic map length (R^2 = 0.99; P < 0.001, Fig. 2A, Supplementary Information Table S1). However, recombination density showed a negative logarithmic relationship with SC size (R^2 = 0.77; P < 0.001) (Fig. 2B, Table S1),

indicating that smaller chromosomes have higher mean recombination rates, despite the fact that larger chromosomes have a higher total number of crossovers.

Sex chromosomes formed heteromorphic synaptonemal complexes. The Z chromosome was a large submetacentric (arm ratio = 2.1), and the W chromosome was a medium subtelocentric (arm ratio = 5.0). Their axial elements varied in size and shape depending on synaptic configuration. In a fraction of pachytene cells where most autosomes were completely synapsed, we observed co-localized but not yet paired Z and W chromosomes (Fig. 1B), as these cells appeared to be at the early pachytene substage. Pairing between the Z and W chromosomes was usually initiated at the ends of their short arms (Zp and Wp). However, in some cells, the ends of their long arms (Zq and Wq) were also paired (Fig. 1C, F, G). Most pachytene cells contained Z and W chromosomes paired along the whole length of their short arms and almost along the whole length of Wq. The ZpWp pairing region almost always contained a single MLH1 focus at the very distal part. The average distance between the telomeres and the MLH1 focus in this region was 1.2 ± 0.3 μm ranging from 0.6 to 1.8 μm or 23% of Wp (Fig. 1D–F). We can estimate the approximate size of the region where recombination occurs (pseudoautosomal region) as the distance between the most proximal and the most distal positions of the MLH1 foci (1.2 μm). This means that the pseudoautosomal region of ZW in the wagtail is much smaller than the ZpWp pairing region. We did not observe MLH1 foci at the second pairing region of ZqWq. Synaptic adjustment of the sex chromosomes involved a shortening of the Zp chromosome (to approximately 67% of its length in the unpaired state). Wp was elongated by 125% when the pairing extended up to its centromere and by 195% when it was completely paired with Z. Zq remained the same length in unpaired and paired states, while Wq elongated by 142% when paired. Complete synapsis between Z and W was achieved in two ways. In one group of cells, Z was twisted around W (Fig. 1E). In other group of cells (24%; 35 out of 147 cells), we observed synapsis at both ends of the sex chromosomes: the whole Wp and a proximal part of Wq with Zp; the distal part of Wq with the distal part of Zq; and one or more D-loops in the medial part of Zq (Fig. 1F, G). This configuration is likely to occur over the course of synaptic adjustment of configurations similar to that shown in Figure 1C.

DISCUSSION

Using a precise and easily comparable cytological approach, we analysed meiotic recombination in the white wagtail – a bird species where closely related populations show striking contrast between plumage variation and patterns in genetic markers (Semenov *et al.*, 2017, 2018). We hypothesized that along with selection on plumage traits and gene flow between the subspecies, a high recombination rate might contribute to this observed pattern. Using the cytological approach described here, we found that the white wagtail has the longest genetic map and the highest crossover rate per autosome set among avian species studied to date, lending support to this hypothesis.

Recombination patterns in the white wagtail and other birds

The record for the highest recombination rate among birds had been held by the domestic chicken (*Gallus gallus*) for a long time. It was hypothesized that this high frequency of crossing over could be due to artificial selection during domestication and might not be representative of other birds (Groenen *et al.*, 2009; Backström *et al.*, 2010). Recently, an even higher recombination rate was found in the greylag goose (*Anser anser*) (Torgasheva & Borodin, 2017), but again in the domesticated form of this species (Table 1). Results of our current study set a new record for the genetic map length known for birds and indicate that exceptionally high recombination rates exist among wild avian taxa. Of particular note, these findings resurrect the question of whether the rate of meiotic recombination is generally higher in birds compared to other vertebrates (International Chicken Genome Sequencing Consortium, 2004), due to a higher proportion of microchromosomes and the relatively small size of avian genomes.

A previous study identified a strong negative relationship between the physical size of chromosomes and the rate of recombination in birds and mammals (Backström *et al.*, 2010). Although larger chromosomes tend to have more crossovers, crossover density is higher in smaller chromosomes, resulting in an increased mean recombination rate (e.g. in the collared flycatcher (*Ficedula albicollis*): Kawakami *et al.*, 2014). Our observations in the white wagtail were consistent with this pattern (Fig. 2A, B, Table S1). Interestingly, the recombination rate might be substantially higher at microchromosomes in the white wagtail compared to other bird species. In the domestic chicken, individual macrobivalents had approximately the same average MLH1 number as in the white wagtail [total numbers of crossovers in SC1–8 are 34.2 and 34.5 in the wagtail and the chicken (Pigozzi, 2001), respectively]. However, the wagtail microchromosomes had about one-quarter more crossovers than their chicken homologues (42.2 and 31.2, respectively). Despite the fact that a single

crossover on a microchromosome would shuffle fewer functional genetic elements compared to a crossover on a macrochromosome, all else being equal, gene density might be approximately doubled in the microchromosomes of birds (Smith *et al.*, 2000). The evolutionary effects of this peculiarity of the white wagtail genome warrant further investigation.

Recent studies have shown that most eukaryotes exhibit a reduced crossover rate in chromosome centres relative to chromosome peripheries – an important finding for interpreting heterogeneous genomic patterns of population differentiation (Berner & Roesti, 2017; Haenel *et al.*, 2018). In the zebra finch (*Taeniopygia guttata*), the only passerine bird with known MLH1 macrochromosome maps, both cytological and genetic mapping indicated that the reduction of recombination rates in macrochromosome centres is more extreme than in other birds (Calderón & Pigozzi, 2006; Backström *et al.*, 2010). Some of the zebra finch macrochromosomes demonstrated a complete absence of crossovers over about two-thirds of the internal chromosome fraction (Calderón & Pigozzi, 2006). This pattern of recombination hotspots and vast recombination 'deserts' was further evident in the zebra finch and another estrildid species, the long-tailed finch (*Poephila acuticauda*), based on analysis of genome-wide linkage disequilibrium data (Singhal *et al.*, 2015). The white wagtail macrochromosomes exhibited a clear U-shaped distribution of crossover frequencies (Fig. 2), adding another example of comparatively reduced recombination in the chromosome centres. However, with the exception of a narrow region of suppressed recombination near centromeres, crossovers occurred along the entire length of chromosomes in the white wagtail. The recombination landscapes of the white wagtail therefore did not exhibit the pronounced recombination 'deserts' observed in some estrildids [see our Figs 2 and fig. 3 in Calderón & Pigozzi (2006) for comparison], and were similar to those described in the majority of other birds: Japanese quail (*Coturnix japonica*) (del Priore & Pigozzi, 2015), domestic duck (*Anas platyrhynchos*) (Pigozzi & del Priore, 2016), greylag goose (*Anser anser*) (Torgasheva & Borodin, 2017), domestic pigeon (*Columba livia*) (Pigozzi & Solari, 1999a), domestic chicken (*Gallus gallus*) (Groenen *et al.*, 2009) and collared flycatcher (*Ficedula albicollis*) (Kawakami *et al.*, 2014).

In Palaeognathae, the Z and W chromosomes are almost identical genetically and morphologically (Zhou *et al.*, 2014). They pair and recombine freely along their whole lengths with the exception of a very terminal region on the Z chromosome. Neognathae species vary in their degree of genetic and morphological divergence between the Z and the W chromosomes (Zhou *et al.*, 2014). However, all species examined so far have shown a uniform pattern of Z–W pairing and recombination. Their Z and W chromosomes pair homologously over a very short region and then undergo extensive equalization of their axes forming almost homomorphic SCs. A single recombination event always occurs in the region of pairing initiation (Solari, 1992; Solari & Pigozzi, 1993; Pigozzi & Solari, 1999a; Pigozzi, 2001). Patterns of Z and W chromosome pairing and synaptic adjustment in the white wagtail were to some extent similar to those described in other Neognathae: in most cells, the Z and W chromosomes paired homologously and formed a single crossover in a distal region of SCs (Fig. 1D, E) (Solari, 1992; Solari & Pigozzi, 1993; Pigozzi & Solari, 1999a). However, the second pairing region which we detected in one-quarter of pachytene cells examined (Fig. 1C, F, G) has not been observed in other bird species, although it has been reported in several species of mammals [e.g. in humans (Graves *et al.*, 1998) and the Mandarin vole *Microtus mandarinus* (Borodin *et al.*, 2012). It is unclear whether synapsis in this region is homologous or not. An absence of MLH1 foci in the second pairing region might be due to a lack of homology or epigenetic suppression of recombination anywhere beyond the main pseudoautosomal region. If the second pairing region between Z and W is homologous, it is more likely to be a result of a translocation from autosomes than a relic of ancient homology, because only one pairing region was detected in other Neognathae. Additional studies are needed to clarify the nature of this chromosomal region.

Despite increasing interest in the role of recombination variation within and across taxa (Payseur, 2016; Dapper & Payseur, 2017; Stapley *et al.*, 2017b), such comparative studies remain challenging. In part, this is because recombination patterns have been examined for a relatively small set of taxa in most taxonomic groups. Another challenge is presented by the difficulties of comparing estimates of recombination inferred using different methods. Estimates from linkage studies depend critically on the number and location of markers used. Low-density mapping and the lack of markers in some chromosome segments (especially in subtelomeric regions) can underestimate the genetic length of individual chromosomes and the whole genome. For example, the length of the high-density genetic map of female chickens (3098 cM: Groenen *et al.*, 2009) was similar to that of the MLH1-based map (3251 cM: Pigozzi, 2001). In contrast, the low-density sex-averaged genetic maps of zebra finch estimated as 1068 cM by Stapley *et al.* (2008) and 1341 cM by Backström *et al.* (2010), were about two times shorter than the MLH1-based map of 2273 cM (Calderón & Pigozzi, 2006). With the exception of the zebra finch, all other passerine recombination maps come from linkage studies (Table 1) and may thus underestimate recombination rate. We therefore stress the advantages of the cytological framework for future comparative research.

Implications of high recombination rate for speciation patterns observed in the white wagtail

The shortcomings associated with comparing estimates of recombination rates derived from different methods warrant caution when comparing our data with others. Nonetheless, the recombination features observed in the white wagtail probably contribute to the pattern of morphological differences coexisting with shallow genomic differentiation and discordant plumage and phylogeographical patterns that have been observed in this species. First, a high recombination rate could impede lineage sorting between geographically remote populations and enhance the homogenizing effects of gene flow between adjacent ones. In addition, the large population size of the white wagtail (130–230 million individuals, http://datazone.birdlife.org) could amplify such effects due to the negative association between effective population size and the rate of genetic drift (Pease & Hahn, 2013). These ideas are consistent with the pattern of shallow divergence in nuclear molecular markers and comparatively higher divergence in non-recombinant mtDNA across the white wagtail range (Pavlova *et al.*, 2005; Li *et al.*, 2016; Semenov *et al.*, 2017; Harris *et al.*, 2018). Second, unlike some species with extremely uneven recombination landscapes, crossovers were distributed along the majority of chromosomal arm lengths in wagtails (Fig. 2), which could enhance genetic homogenization. Finally, a high recombination rate could contribute to shrinking the size of haplotype blocks affected by selection and promote decoupling between evolutionary processes influencing plumage traits and selectively neutral genetic variation. This hypothesis should be further addressed by assessing fine-scale recombination patterns in the genome with respect to regions underlying plumage differences.

Hybridization is pervasive among white wagtail subspecies (Fig. 1). In the face of gene flow, recombination can impose constraints on the genetic architecture of traits involved in reproductive barriers (Feder *et al.*, 2012; Feder *et al.*, 2013). As recombination breaks down associations between alleles at different loci, traits with simpler genetic architecture may have a higher likelihood of playing a role in reproductive barriers (Coyne & Orr, 2004; Flaxman *et al.*, 2014), implying that selection may preferably target such traits. Indeed, in a hybrid zone between the *alba* and *personata* white wagtail subspecies, the plumage trait with the simplest segregation pattern is the only one probably maintained by selection (Semenov *et al.*, 2017). It therefore appears plausible that high rates of meiotic recombination could contribute to multiple aspects of white wagtail evolution.

CONCLUSIONS

In summary, we found that the white wagtail – a species with striking contrast between well-delineated intraspecific plumage divergence and a lack of corresponding genetic differentiation – has several parameters of meiotic recombination that are highest among all bird species studied to date. Although our findings suggest that variation in recombination rates might contribute to distinct speciation patterns across taxa, the limited amount of comparative data makes it difficult to derive general conclusions. It remains unknown how common it is to find elevated rates of recombination in association with patterns of extensive phenotypic diversification yet shallow genomic divergence. There are a number of taxa in which such associations could be expected but have not been assessed (e.g. (Poelstra *et al.*, 2014; Toews *et al.*, 2016; Campagna *et al.*, 2017). A promising avenue of future research would be to compare recombination rates between closely related lineages with and without discordance between morphological and genetic patterns. Our study highlights the importance of studying recombination within a unified methodological framework, which allows direct comparison between independent studies.

ACKNOWLEDGEMENTS

The authors would like to thank David Khaydarov, Irina Malykh and Margarita Valukhina for help with fieldwork, members of the Safran lab for feedback, Yulia Sheina for the wagtail drawings and the Microscopic Center of the Siberian Branch of Russian Academy of Sciences (SB RAS) for granting access to microscopic equipment. We thank two anonymous reviewers for their helpful comments and suggestions. This work was supported by grants from the Russian Foundation for Basic Research (16-04-00087 and 18-04-00924) and The Federal Agency for Scientific Organizations via the Institute of Cytology and Genetics (0324-2018-0019). Sampling was conducted in accordance with Russian and international guidelines for the use of animals and was approved by the Ethics Committee on Animal Care and Use of the ICG SB RAS (No. 35: 10/26/2016). The authors have no conflicts of interest to declare.

REFERENCES

Åkesson M, Hansson B, Hasselquist D, Bensch S. 2007. Linkage mapping of AFLP markers in a wild population of great reed warblers: importance of heterozygosity and number of genotyped individuals. *Molecular Ecology* **16:** 2189–2202.

Anderson LK, Reeves A, Webb LM, Ashley T. 1999. Distribution of crossing over on mouse synaptonemal complexes using immunofluorescent localization of MLH1 protein. *Genetics* **151:** 1569–1579.

Aslam ML, Bastiaansen JW, Crooijmans RP, Vereijken A, Megens HJ, Groenen MA. 2010. A SNP based linkage map of the turkey genome reveals multiple intrachromosomal rearrangements between the turkey and chicken genomes. *BMC Genomics* **11:** 647.

Backström N, Forstmeier W, Schielzeth H, Mellenius H, Nam K, Bolund E, Webster MT, Ost T, Schneider M, Kempenaers B, Ellegren H. 2010. The recombination landscape of the zebra finch *Taeniopygia guttata* genome. *Genome Research* **20:** 485–495.

Backström N, Karaiskou N, Leder EH, Gustafsson L, Primmer CR, Qvarnström A, Ellegren H. 2008. A gene-based genetic linkage map of the collared flycatcher (*Ficedula albicollis*) reveals extensive synteny and gene-order conservation during 100 million years of avian evolution. *Genetics* **179:** 1479–1495.

Berner D, Roesti M. 2017. Genomics of adaptive divergence with chromosome-scale heterogeneity in crossover rate. *Molecular Ecology* **26:** 6351–6369.

Boopathi NM. 2013. Genetic Mapping and Marker Assisted Selection: Basics, Practice and Benefits. Springer, New York, 293 p. Editor: NA.Chapter: Linkage Map Construction. Chapter pages: 81–108.

Borodin PM, Basheva EA, Torgasheva AA, Dashkevich OA, Golenishchev FN, Kartavtseva IV, Mekada K, Dumont BL. 2012. Multiple independent evolutionary losses of XY pairing at meiosis in the grey voles. *Chromosome Research* **20:** 259–268.

Butlin RK. 2005. Recombination and speciation. *Molecular Ecology* **14:** 2621–2635.

Calderón PL, Pigozzi MI. 2006. MLH1-focus mapping in birds shows equal recombination between sexes and diversity of crossover patterns. *Chromosome Research* **14:** 605–612.

Campagna L, Repenning M, Silveira LF, Fontana CS, Tubaro PL, Lovette IJ. 2017. Repeated divergent selection on pigmentation genes in a rapid finch radiation. *Science Advances* **3:** e1602404.

Campbell CR, Poelstra JW, Yoder AD. 2018. What is speciation genomics? The roles of ecology, gene flow, and genomic architecture in the formation of species. *Biological Journal of the Linnean Society* **124:** 561–583.

Coyne JA, Orr HA. 2004. *Speciation*. Sunderland: Sinauer Associates.

Cutter AD, Payseur BA. 2013. Genomic signatures of selection at linked sites: unifying the disparity among species. *Nature Reviews. Genetics* **14:** 262–274.

Dapper AL, Payseur BA. 2017. Connecting theory and data to understand recombination rate evolution. *Philosophical Transactions of the Royal Society B: Biological Sciences* **372**: pii: 20160469.

Dumont BL, Payseur BA. 2008. Evolution of the genomic rate of recombination in mammals. *Evolution* **62:** 276–294.

Feder JL, Egan SP, Nosil P. 2012. The genomics of speciation-with-gene-flow. *Trends in Genetics* **28:** 342–350.

Feder JL, Flaxman SM, Egan SP, Comeault AA, Nosil P. 2013. Geographic mode of speciation and genomic divergence. *Annual Review of Ecology, Evolution, and Systematics* **44:** 73–97.

Flaxman SM, Wacholder AC, Feder JL, Nosil P. 2014. Theoretical models of the influence of genomic architecture on the dynamics of speciation. *Molecular Ecology* **23:** 4074–4088.

Graves JA, Wakefield MJ, Toder R. 1998. The origin and evolution of the pseudoautosomal regions of human sex chromosomes. *Human Molecular Genetics* **7:** 1991–1996.

Groenen MA, Wahlberg P, Foglio M, Cheng HH, Megens HJ, Crooijmans RP, Besnier F, Lathrop M, Muir WM, Wong GK, Gut I, Andersson L. 2009. A high-density SNP-based linkage map of the chicken genome reveals sequence features correlated with recombination rate. *Genome Research* **19:** 510–519.

Haddrill PR, Halligan DL, Tomaras D, Charlesworth B. 2007. Reduced efficacy of selection in regions of the Drosophila genome that lack crossing over. *Genome Biology* **8:** R18.

Haenel Q, Laurentino TG, Roesti M, Berner D. 2018. Meta-analysis of chromosome-scale crossover rate variation in eukaryotes and its significance to evolutionary genomics. *Molecular Ecology* **27:** 2477–2497.

Hansson B, Ljungqvist M, Dawson DA, Mueller JC, Olano-Marin J, Ellegren H, Nilsson JA. 2010. Avian genome evolution: insights from a linkage map of the blue tit (*Cyanistes caeruleus*). *Heredity* **104:** 67–78.

Harris RB, Alström P, Ödeen A, Leaché AD. 2018. Discordance between genomic divergence and phenotypic variation in a rapidly evolving avian genus (*Motacilla*). *Molecular Phylogenetics and Evolution* **120:** 183–195.

Hill WG, Robertson A. 1966. The effect of linkage on limits to artificial selection. *Genetical Research* **8:** 269–294.

Howell WM, Black DA. 1980. Controlled silver-staining of nucleolus organizer regions with a protective colloidal developer: a 1-step method. *Experientia* **36:** 1014–1015.

Huang CW, Cheng YS, Rouvier R, Yang KT, Wu CP, Huang HL, Huang MC. 2009. Duck (*Anas platyrhynchos*) linkage mapping by AFLP fingerprinting. *Genetics, Selection, Evolution* **41:** 28.

International Chicken Genome Sequencing Consortium. 2004. Sequence and comparative analysis of the chicken genome provide unique perspectives on vertebrate evolution. *Nature* **432:** 695–716.

Jaari S, Li MH, Merilä J. 2009. A first-generation microsatellite-based genetic linkage map of the Siberian jay (*Perisoreus infaustus*): insights into avian genome evolution. *BMC Genomics* **10:** 1.

Kawakami T, Mugal CF, Suh A, Nater A, Burri R, Smeds L, Ellegren H. 2017. Whole-genome patterns of linkage disequilibrium across flycatcher populations clarify the causes and consequences of fine-scale recombination rate variation in birds. *Molecular Ecology* **26:** 4158–4172.

Kawakami T, Smeds L, Backström N, Husby A, Qvarnström A, Mugal CF, Olason P, Ellegren H. 2014. A high-density linkage map enables a second-generation collared flycatcher genome assembly and reveals the patterns of avian recombination rate variation and chromosomal evolution. *Molecular Ecology* **23:** 4035–4058.

Kikuchi S, Fujima D, Sasazaki S, Tsuji S, Mizutani M, Fujiwara A, Mannen H. 2005. Construction of a genetic linkage map of Japanese quail (*Coturnix japonica*) based on AFLP and microsatellite markers. *Animal Genetics* **36:** 227–231.

Kondrashov AS. 1988. Deleterious mutations and the evolution of sexual reproduction. *Nature* **336:** 435–440.

Li X, Dong F, Lei F, Alström P, Zhang R, Ödeen A, Fjeldså J, Ericson PGP, Zou F, Yang X. 2016. Shaped by uneven Pleistocene climate: mitochondrial phylogeographic pattern and population history of white wagtail *Motacilla alba* (Aves: Passeriformes). *Journal of Avian Biology* **47:** 263–274.

Lisachov A, Malinovskaya L, Druzyaka AV, Borodin PM, Torgasheva AA. 2017. Synapsis and recombination of autosomes and sex chromosomes in two terns (Sternidae, Charadriiformes, Aves). *Vavilovskii Zhurnal Genetiki i Selektsii* **21:** 259–268.

Malinovskaya L, Shnaider E, Borodin PM, Torgasheva AA. 2018. Karyotypes and recombination patterns of the Common Swift (*Apus apus* Linnaeus, 1758) and Eurasian Hobby (*Falco subbuteo* Linnaeus, 1758). *Avian Research* **9:** 4.

Mueller JC. 2004. Linkage disequilibrium for different scales and applications. *Briefings in Bioinformatics* **5:** 355–364.

Muller HJ. 1964. The relation of recombination to mutational advance. *Mutation Research* **106:** 2–9.

Nietlisbach P, Camenisch G, Bucher T, Slate J, Keller LF, Postma E. 2015. A microsatellite-based linkage map for song sparrows (*Melospiza melodia*). *Molecular Ecology Resources* **15:** 1486–1496.

Nosil P, Feder JL. 2012. Genomic divergence during speciation: causes and consequences. *Philosophical Transactions of the Royal Society of London. Series B, Biological Sciences* **367:** 332–342.

van Oers K, Santure AW, De Cauwer I, van Bers NE, Crooijmans RP, Sheldon BC, Visser ME, Slate J, Groenen MA. 2014. Replicated high-density genetic maps of two great tit populations reveal fine-scale genomic departures from sex-equal recombination rates. *Heredity* **112:** 307–316.

Ortiz-Barrientos D, Engelstädter J, Rieseberg LH. 2016. Recombination rate evolution and the origin of species. *Trends in Ecology & Evolution* **31:** 226–236.

Pavlova A, Zink RM, Rohwer S, Koblik EA, Red'kin YA, Fadeev IV, Nesterov EV. 2005. Mitochondrial DNA and plumage evolution in the white wagtail *Motacilla alba*. *Journal of Avian Biology* **36:** 322–336.

Payseur BA. 2016. Genetic links between recombination and speciation. *PLoS Genetics* **12:** e1006066.

Pease JB, Hahn MW. 2013. More accurate phylogenies inferred from low-recombination regions in the presence of incomplete lineage sorting. *Evolution* **67:** 2376–2384.

Pengelly RJ, Gheyas AA, Kuo R, Mossotto E, Seaby EG, Burt DW, Ennis S, Collins A. 2016. Commercial chicken breeds exhibit highly divergent patterns of linkage disequilibrium. *Heredity* **117:** 375–382.

Peters AH, Plug AW, van Vugt MJ, de Boer P. 1997. A drying-down technique for the spreading of mammalian meiocytes from the male and female germline. *Chromosome Research* **5:** 66–68.

Pigozzi MI. 2001. Distribution of MLH1 foci on the synaptonemal complexes of chicken oocytes. *Cytogenetics and Cell Genetics* **95:** 129–133.

Pigozzi MI, del Priore L. 2016. Meiotic recombination analysis in female ducks (*Anas platyrhynchos*). *Genetica* **144:** 307–312.

Pigozzi MI, Solari AJ. 1999a. Recombination nodule mapping and chiasma distribution in spermatocytes of the pigeon, *Columba livia*. *Genome* **42:** 308–314.

Pigozzi MI, Solari AJ. 1999b. Equal frequencies of recombination nodules in both sexes of the pigeon suggest a basic difference with eutherian mammals. *Genome* **42:** 315–321.

Pluta AF, Mackay AM, Ainsztein AM, Goldberg IG, Earnshaw WC. 1995. The centromere: hub of chromosomal activities. *Science* **270:** 1591–1594.

Poelstra JW, Vijay N, Bossu CM, Lantz H, Ryll B, Müller I, Baglione V, Unneberg P, Wikelski M, Grabherr MG, Wolf JB. 2014. The genomic landscape underlying phenotypic integrity in the face of gene flow in crows. *Science* **344:** 1410–1414.

del Priore L, Pigozzi MI. 2015. Sex-specific recombination maps for individual macrochromosomes in the Japanese quail (*Coturnix japonica*). *Chromosome Research* **23:** 199–210.

del Priore L, Pigozzi MI. 2017. Broad-scale recombination pattern in the primitive bird *Rhea americana* (Ratites, Palaeognathae). *PLoS ONE* **12:** e0187549.

Reeves A. 2001. MicroMeasure: a new computer program for the collection and analysis of cytogenetic data. *Genome* **44:** 439–443.

Semenov GA, Koblik EA, Red'kin YA, Badyaev AV. 2018. Extensive phenotypic diversification coexists with little genetic divergence and a lack of population structure in the white wagtail subspecies complex (*Motacilla alba*). *Journal of Evolutionary Biology* **31:** 1093–1108.

Semenov GA, Scordato ESC, Khaydarov DR, Smith CCR, Kane NC, Safran RJ. 2017. Effects of assortative mate choice on the genomic and morphological structure of a hybrid zone between two bird subspecies. *Molecular Ecology* **26:** 6430–6444.

Singhal S, Leffler EM, Sannareddy K, Turner I, Venn O, Hooper DM, Strand AI, Li Q, Raney B, Balakrishnan CN, Griffith SC, McVean G, Przeworski M. 2015. Stable recombination hotspots in birds. *Science* **350:** 928–932.

Smith J, Bruley CK, Paton IR, Dunn I, Jones CT, Windsor D, Morrice DR, Law AS, Masabanda J, Sazanov A, Waddington D, Fries R, Burt DW. 2000. Differences in gene density on chicken macrochromosomes and microchromosomes. *Animal Genetics* **31:** 96–103.

Solari AJ. 1992. Equalization of Z and W axes in chicken and quail oocytes. *Cytogenetics and Cell Genetics* **59:** 52–56.

Solari AJ, Pigozzi MI. 1993. Recombination nodules and axial equalization in the ZW pairs of the Peking duck and the guinea fowl. *Cytogenetics and Cell Genetics* **64:** 268–272.

Stack SM, Anderson LK. 2002. Crossing over as assessed by late recombination nodules is related to the pattern of synapsis and the distribution of early recombination nodules in maize. *Chromosome Research* **10:** 329–345.

Stapley J, Birkhead TR, Burke T, Slate J. 2008. A linkage map of the zebra finch *Taeniopygia guttata* provides new insights into avian genome evolution. *Genetics* **179:** 651–667.

Stapley J, Feulner PGD, Johnston SE, et al. 2017a. Recombination: the good, the bad and the variable. *Philosophical Transactions of the Royal Society B: Biological Sciences* **372**: pii: 20170279.

Stapley J, Feulner PGD, Johnston SE, et al. 2017b. Variation in recombination frequency and distribution across eukaryotes: patterns and processes. *Philosophical Transactions of the Royal Society of London. Series B, Biological Sciences* **372:** 20160455.

Stryjewski KF, Sorenson MD. 2017. Mosaic genome evolution in a recent and rapid avian radiation. *Nature Ecology & Evolution* **1:** 1912–1922.

Toews DP, Taylor SA, Vallender R, Brelsford A, Butcher BG, Messer PW, Lovette IJ. 2016. Plumage genes and little else distinguish the genomes of hybridizing warblers. *Current Biology: CB* **26:** 2313–2318.

Torgasheva AA, Borodin PM. 2017. Immunocytological analysis of meiotic recombination in the gray goose (*Anser anser*). *Cytogenetic and Genome Research* **151:** 27–35.

Veller C, Nowak M. 2017. The distribution of crossovers, and the measure of total recombination. *bioRxiv*: doi:10.1101/194837

Westergaard M, von Wettstein D. 1972. The synaptinemal complex. *Annual Review of Genetics* **6:** 71–110.

Wolf JB, Ellegren H. 2017. Making sense of genomic islands of differentiation in light of speciation. *Nature Reviews Genetics* **18:** 87–100.

Zhou Q, Zhang J, Bachtrog D, An N, Huang Q, Jarvis ED, Gilbert MT, Zhang G. 2014. Complex evolutionary trajectories of sex chromosomes across bird taxa. *Science* **346:** 1246338.

SUPPORTING INFORMATION

Additional Supporting Information may be found in the online version of this article at the publisher's website.

Table S1. Synaptonemal complex (SC) length, MLH1 foci number per bivalent and estimates of genetic distance and recombination rate of the white wagtail female bivalents ranked by their relative size in each cell. ZW indicates the pseudoautosomal region of ZW chromosome SC.